

# H/D Exchange and Isomerization of Small Alkanes over Unpromoted and Al<sub>2</sub>O<sub>3</sub>-Promoted SO<sub>4</sub><sup>2-</sup>/ZrO<sub>2</sub> Catalysts

Weiming Hua, Alain Goeppert, and Jean Sommer<sup>1</sup>

Laboratoire de Physico-Chimie des Hydrocarbures, Institut de Chimie, Université Louis Pasteur,  
4 rue Blaise Pascal, F-67070 Strasbourg Cedex, France

Received September 4, 2000; revised October 30, 2000; accepted October 30, 2000; published online January 10, 2001

The H/D exchange reaction between methane and deuterated SZ, SZ/Al<sub>2</sub>O<sub>3</sub>, and SZA catalysts was studied. The apparent activation energy on SZ/Al<sub>2</sub>O<sub>3</sub> and SZA catalysts is the same as that on SZ, but substantially smaller than that on HZSM-5 zeolite, indicating that the acid strengths of Al<sub>2</sub>O<sub>3</sub>-promoted SZ catalysts are identical to that of SZ, but stronger than that of HZSM-5. The catalytic properties of unpromoted and Al<sub>2</sub>O<sub>3</sub>-promoted SZ for the isomerization of *n*-butane and isobutane at 250°C in the presence of H<sub>2</sub> were investigated. These catalysts deactivate more slowly during isobutane isomerization than during *n*-butane isomerization. The rate of isobutane conversion is lower than that of *n*-butane isomerization for the same sulfated zirconia-based catalyst. The rates of *n*-butane and isobutane conversion are all in the sequence of SZA > SZ/Al<sub>2</sub>O<sub>3</sub> > SZ, the same as that for the H/D exchange of methane over these catalysts. © 2001 Academic Press

**Key Words:** H/D exchange; methane; Al<sub>2</sub>O<sub>3</sub>-promoted SZ; strong acids; superacids; isomerization of *n*-butane and isobutane; alkane activation.

## 1. INTRODUCTION

Acid-catalyzed hydrocarbon conversions, such as catalytic cracking, isomerization, and alkylation, are large-scale industrial processes that play a key role in the petrochemical industry (1). To overcome the chemical inertness of the starting material, high-temperature and/or strongly acidic catalysts are generally employed. Sulfated zirconia (SZ) and related materials have often been assigned superacidic (2) properties due to their unique catalytic activity and selectivity for light *n*-alkanes isomerization at low temperature. Therefore, a considerable number of reports dealing with SZ and its analogues have appeared since the original report by Hino *et al.* (3), and significant interest in this new type of catalytic material is well reflected in the regularly published reviews (4–9).

In the early 1990s, Hsu *et al.* (10, 11) first discovered that, at low temperature, sulfated zirconia promoted with

Fe and Mn (SFMZ) is 2–3 orders of magnitude more active in *n*-butane isomerization than unpromoted SZ. Following this observation, recent studies on sulfated oxides have concentrated on the transition-metals-promoted SZ catalysts. However, these catalysts deactivate rapidly during the isomerization of *n*-butane, e.g., the Fe- and Mn-promoted catalyst deactivates quickly at 60°C in the presence of N<sub>2</sub> or at 250°C in the presence of H<sub>2</sub> (12, 13). More recently, Gao *et al.* (14, 15) have found that the addition of Al into SZ (SZA) or supporting SZ over  $\gamma$ -Al<sub>2</sub>O<sub>3</sub> (SZ/Al<sub>2</sub>O<sub>3</sub>) enhances significantly the activity and stability of the catalysts for *n*-butane isomerization at 250°C in the presence of H<sub>2</sub>. The promoting mechanism of the main group element Al is different from that of transition metals.

For the understanding of catalytic hydrocarbon conversion over acidic catalysts, there is, however, a strong contrast between the general agreement on the role of carbocations as intermediates and the lack of information on their mode of formation. Among saturated hydrocarbons methane is the weakest base and the most thermodynamically stable alkane. Recently, Schoofs *et al.* (16) have studied the H/D exchange reaction between methane and acidic FAU- and MFI-type zeolites. Structural (FAU vs MFI) and chemical (Si/Al ratio) effects on the reaction kinetics were established. In the present paper we report our investigation of the H/D exchange reaction of methane over unpromoted and Al<sub>2</sub>O<sub>3</sub>-promoted SZ catalysts in comparison with HZSM-5 (Si/Al = 39) zeolite. *n*-Butane and isobutane isomerization over these catalysts at high temperature in the presence of hydrogen have also been studied and compared.

## 2. EXPERIMENTAL

### Catalysts

#### 2.1. Catalyst Preparation

SO<sub>4</sub><sup>2-</sup>/ZrO<sub>2</sub>, SO<sub>4</sub><sup>2-</sup>/Al<sub>2</sub>O<sub>3</sub>-ZrO<sub>2</sub>, and SO<sub>4</sub><sup>2-</sup>/ZrO<sub>2</sub>/ $\gamma$ -Al<sub>2</sub>O<sub>3</sub> were previously described in the literature (14, 15, 17, 18). We have slightly modified their preparation as follows:

<sup>1</sup> To whom correspondence should be addressed. Fax: 33 (0)3 88 45 46 47. E-mail: [sommer@chimie.u-strasbg.fr](mailto:sommer@chimie.u-strasbg.fr).

$\text{SO}_4^{2-}/\text{Al}_2\text{O}_3\text{-ZrO}_2$ . An aqueous solution of ammonia was added dropwise under vigorous stirring at room temperature to a mixed solution of  $\text{ZrOCl}_2 \cdot 8\text{H}_2\text{O}$  and  $\text{Al}(\text{NO}_3)_3 \cdot 9\text{H}_2\text{O}$  up to a pH of 9–10. The precipitate was then filtered and washed with deionized water until there were no detectable chlorine ions in the washing water. After the mixed hydroxide was dried at  $110^\circ\text{C}$  for 24 h, it was immersed in a 1 N  $\text{H}_2\text{SO}_4$  solution at a ratio of 15 ml/g of hydroxide and left for 1 h with continuous stirring at room temperature to reach equilibrium. The sulfated  $\text{Al}(\text{OH})_3\text{-Zr}(\text{OH})_4$  was then filtered without washing, drying at  $110^\circ\text{C}$  for 24 h, and calcined at  $650^\circ\text{C}$  under static air for 3 h. The obtained catalyst containing 3.0 mol%  $\text{Al}_2\text{O}_3$  was designated **SZA**.

$\text{SO}_4^{2-}/\text{ZrO}_2$ . This catalyst which was labelled as **SZ** was prepared in the same way as SZA by immersing  $\text{Zr}(\text{OH})_4$  in a 1 N  $\text{H}_2\text{SO}_4$  solution, followed by calcination at  $650^\circ\text{C}$  under static air for 3 h.

$\text{SO}_4^{2-}/\text{ZrO}_2/\gamma\text{-Al}_2\text{O}_3$ . A solution of ammonia in deionized water was added dropwise under vigorous stirring at room temperature to a solution of  $\text{ZrO}(\text{NO}_3)_2$  containing  $\gamma\text{-Al}_2\text{O}_3$  (>400 mesh) as a core matrix in suspension. The obtained precipitate was then treated as described above. The catalyst containing 90 wt%  $\text{ZrO}_2$  was named **SZ/Al<sub>2</sub>O<sub>3</sub>**.

HZSM-5 zeolite (Si/Al=39) was from P.Q. Corp. CBV8020. Prior to use, this ammonium form zeolite was calcinated at  $500^\circ\text{C}$  for 8 h to obtain the proton form.

## 2.2. Surface Area and Sulfur Content

BET surface areas of the samples were performed on a Micromeritics ASAP 2000 system. The sulfur content in the catalysts was measured at Service Central d'Analyse du CNRS, Vernaison, Lyon.

## Experimental Procedures

All reactions, such as deuteration of the catalyst, Brønsted acid sites titration, the H/D exchange reaction between the catalyst and methane, and activity test were performed in an all-glass grease-free flow system described earlier (19).

## 2.3. Deuteration of the Catalyst

The catalyst was first activated under dry air at  $450^\circ\text{C}$  for 2 h to eliminate hydrocarbon contamination. Then, it was pretreated with dry He at the same temperature for an additional 1 h. The temperature was lowered to  $200^\circ\text{C}$ , and the catalyst was deuterated by sweeping  $\text{D}_2\text{O}$  with He (40 ml  $\text{min}^{-1}$ , ca. 3 mol%  $\text{D}_2\text{O}$  in He) for 1.5 h. Excess  $\text{D}_2\text{O}$  was then removed by flushing the catalyst at  $450^\circ\text{C}$  with dry He for 1 h.

## 2.4. Procedure for H/D Exchange

The H/D exchange reaction between methane and the deuterated catalyst was performed in a recirculation reactor. The loading for sulfated zirconia-based catalysts was 2 and 1 g for HZSM-5. In each run 2 ml of methane was injected into the closed system containing the deuterated catalyst and helium to keep the amount of methane hydrogen atoms and deuterium atoms present on the catalyst in the same order of magnitude. The reactor was first recirculated in bypass mode without contact between methane and the catalyst to ensure a good mixing of the gases. The methane fragmentation pattern was measured to correct the *m/z* signals of isotopomers of methane. After stabilization of the temperature in the desired range 325 to  $450^\circ\text{C}$ , methane was contacted with the catalyst, and deuteration was followed by GC-MS as a function of time.

## 2.5. Acid Site Density

The above deuterated catalyst (1 g) was contacted at  $200^\circ\text{C}$  for 1.5 h with He (40 ml  $\text{min}^{-1}$ , ca. 3 mol%  $\text{H}_2\text{O}$  in He) bubbled through a U tube containing distilled  $\text{H}_2\text{O}$  at room temperature. Excess water was then removed by flushing the catalyst at  $450^\circ\text{C}$  for 1 h with dry He. During the H/D exchange and flushing, the partially exchanged water ( $\text{H}_2\text{O}/\text{HDO}/\text{D}_2\text{O}$  mixture, named  $\text{H}_x\text{OD}_y$ ) was collected in a cold trap. An excess of trifluoroacetic anhydride was then added to  $\text{H}_x\text{OD}_y$  trapped. The acid solution thus obtained was analyzed by 400 MHz  $^1\text{H}$  and  $^2\text{H}$  NMR after addition of a  $\text{CDCl}_3/\text{CHCl}_3$  mixture used as the internal standard. The acid site density was then calculated based on the H/D ratio determined by NMR and the weight of  $\text{H}_x\text{OD}_y$  condensed.

## 2.6. Activity Test

A gas mixture of *n*-butane and  $\text{H}_2$  (1:10 molar ratio) or isobutane and  $\text{H}_2$  (1:10 molar ratio) was passed at a rate of 22.8 ml  $\text{min}^{-1}$  over the catalyst (0.4 g) at  $250^\circ\text{C}$  under ambient pressure. Prior to the reaction, the catalyst was pretreated *in situ* in dry air at  $450^\circ\text{C}$  for 3 h. Analysis of the effluent gas from the reactor was performed on a Girdel 300 with an FID detector using a 2-m packed column HAYESED R, and the temperature of the oven was kept at  $130^\circ\text{C}$ .

## 3. RESULTS AND DISCUSSION

### 3.1. Catalyst Characterization

The surface area, sulfur content, and Brønsted acid sites of the catalysts are compiled in Table 1. BET surface areas of both **SZ/Al<sub>2</sub>O<sub>3</sub>** and **SZA** are identical within the experimental deviation, which are ca. 30% greater than that of the **SZ** catalyst, showing that addition of  $\text{Al}_2\text{O}_3$  helps to preserve the surface area of **SZ**. The sulfur content of **SZ/Al<sub>2</sub>O<sub>3</sub>**

TABLE 1  
Properties of Various Catalysts

Catalyst	Surface area (m <sup>2</sup> g <sup>-1</sup> )	Sulfur content (wt%)	Brønsted sites (mmol g <sup>-1</sup> )
SZ	96.9	1.03	0.0645
SZ/Al <sub>2</sub> O <sub>3</sub>	128.9	1.62	0.136
SZA	134.4	1.47	0.121
HZSM-5	450.0	—	0.417 <sup>a</sup>

<sup>a</sup> Corresponding to the number of Al atoms.

is slightly higher than that of SZA, and both catalysts possess significantly higher sulfur content than SZ, indicating that the addition of Al<sub>2</sub>O<sub>3</sub> into or onto SZ helps to stabilize the surface sulfate complexes remarkably. The above results are analogous to those reported in the literature (14, 15). In the case of Brønsted acid sites on sulfated zirconia-based catalysts, they are very much similar to the feature for sulfur content.

Damyannova *et al.* (20) prepared silica- and alumina-supported zirconia samples by a modified impregnation method. A strong interaction was observed between zirconia and the support due to the formation of Zr–O–Al and Zr–O–Si bonds on the surface of ZrO<sub>2</sub>/Al<sub>2</sub>O<sub>3</sub> and ZrO<sub>2</sub>/SiO<sub>2</sub> binary oxides. Djuricic and co-workers (21) studied the influence of Zr dopant on the thermal stability of alumina. In this ZrO<sub>2</sub>–Al<sub>2</sub>O<sub>3</sub> chemical mixed oxide synthesized by the coprecipitation method, Al–O–Zr bridges are believed to exist resulting from the incorporation of Zr dopant into the lattice structure of alumina. Referring to the above reported results, we think that the formation of Zr–O–Al bonds in both SZ/Al<sub>2</sub>O<sub>3</sub> and SZA samples may help to stabilize more surface sulfate complexes, as seen in Table 1. Consequently, much more Brønsted acid sites are produced over SZ/Al<sub>2</sub>O<sub>3</sub> and SZA than over SZ.

### 3.2. H/D Exchange of Methane over Unpromoted and Al<sub>2</sub>O<sub>3</sub>-Promoted SZ Catalysts

The concentration of methane isotopomers (CH<sub>x</sub>D<sub>4-x</sub> with  $x = 0-4$ ) must be related to the intensity of their respective molecular ion peaks analyzed by GC-MS. To estimate the contribution of each methane isotopolog to the mass spectra, a correction is needed due to the superposition of various fragmentation peaks. The correction method is based on the work of Schoofs and co-workers (16), viz., the degree of fragmentation for all the methane isotopomers is supposed to be the same. The fragmentation pattern of unreacted methane can be determined when the recirculation reactor was run in bypass mode.

For an experiment on a SZ catalyst at 450°C, after the mass spectral corrections the real distribution of methane isotopomers (mol%) is obtained, and the results are presented in Fig. 1. It can be seen from Fig. 1 that the mono-,

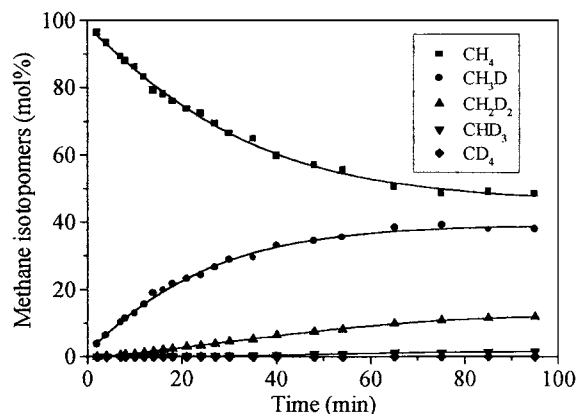


FIG. 1. Distribution of the methane isotopomers (mol%) as a function of time for an experiment on a SZ catalyst at 450°C.

bis-, ter-, and per-deuterated isotopomers of methane are formed in a consecutive way: CH<sub>4</sub> → CH<sub>3</sub>D → CH<sub>2</sub>D<sub>2</sub> → CHD<sub>3</sub> → CD<sub>4</sub>. The concentration of CH<sub>4</sub> decreases gradually with time, whereas the concentration of deuterated products increases. The mono-deuterated product is first formed. As the catalyst is gradually depleted of deuterium, the more deuterated products are generated. Similar features are observed on SZ/Al<sub>2</sub>O<sub>3</sub> and SZA samples (not shown). For comparison, HZSM-5 zeolite was investigated, and it was found that the deuterated products were formed also in a consecutive way (not shown), which is in good agreement with the results of Schoofs *et al.* (16). In summary, the H/D exchange of methane over both sulfated zirconia-based catalysts and HZSM-5 zeolite is stepwise via the exchange of one H/D atom at a time.

The rate of H/D exchange between methane and deuterated catalysts is determined from the slope of the straight line that is obtained when the amount of deuterium incorporated into methane is plotted versus time, and the H/D exchange data of the initial reaction period are taken to be linearly fitted, as shown in Fig. 2. As expected, the H/D

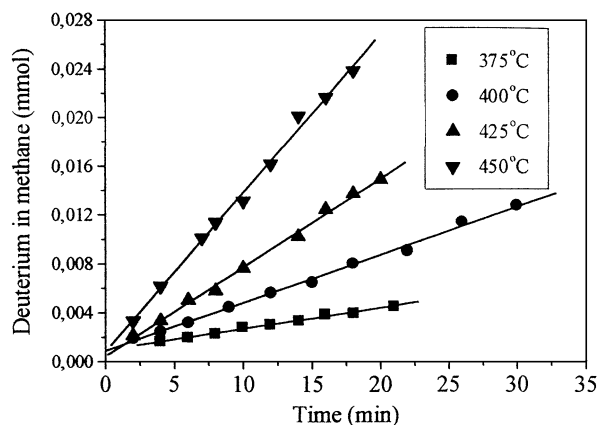


FIG. 2. H/D exchange rate of methane over a deuterated SZ catalyst at different temperatures.

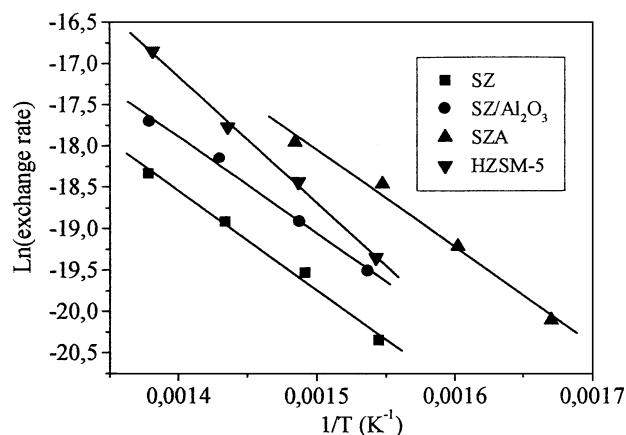


FIG. 3. Arrhenius plot for the H/D exchange of methane on deuterated catalysts.

exchange rate over SZ increases with the reaction temperature. Based on the kinetic data in Fig. 2, the apparent activation energy can be estimated from the slope of the Arrhenius plot. Figure 3 presents the Arrhenius plot of the exchange rate versus temperature for both sulfated zirconia-based catalysts and HZSM-5, and the H/D exchange kinetic parameters are summarized in Table 2.

Since the H/D exchange between alkanes and solid acids is an acid-catalyzed reaction, the experimental H/D exchange results must be related to solid acidities. It can be seen from Table 2 that the exchange rate of methane over sulfated zirconia-based catalysts is in the order of  $SZA > SZ/Al_2O_3 > SZ$ . Both SZA and  $SZ/Al_2O_3$  catalysts have much more Brønsted acid sites than SZ. The former two catalysts are, therefore, much more active than the latter for the H/D exchange of methane. The difference between the H/D exchange rate of methane and Brønsted acid site density on SZA and  $SZ/Al_2O_3$  samples may be caused by the different acid strength distributions over these two samples. Based on microcalorimetric results (14), it has been observed that the total number of acid sites on SZA is 1.6 times larger than that on SZ, whereas the number of intermediate strong acid sites of the former is 4.3 times

greater than that of the latter. The lower H/D exchange rate of methane over HZSM-5 in contrast to its much larger number of Brønsted acid sites implies that the acidity of HZSM-5 may be less than those of SZ,  $SZ/Al_2O_3$ , and SZA samples.

Theoretical calculations have also shown that the hydron exchange rate between methane and a zeolite cluster was directly related to the proton donating ability of the catalyst (41). Within experimental error, the apparent activation energy is identical to that of SZ,  $SZ/Al_2O_3$ , and SZA samples. That is around  $95 \text{ kJ mol}^{-1}$ . On HZSM-5 zeolite, it is ca.  $130 \text{ kJ mol}^{-1}$ , 35% higher than that on sulfated zirconia-based catalysts. To obtain the absolute activation energy, the adsorption heat of methane over these samples has to be accounted for. On MFI-type zeolites this adsorption heat is around  $22 \text{ kJ mol}^{-1}$  as reported by Eder *et al.* (22), leading to an absolute activation energy of  $151 \text{ kJ mol}^{-1}$  on HZSM-5. In zeolite micropores, the larger energetic interactions between the adsorbed alkane molecules and the force field of the zeolite depend strongly on the pore shape and diameter, and the adsorption heat of a particular alkane increases with decreasing the pore size of zeolite (22–26). Although the adsorption heat of methane over unpromoted and  $Al_2O_3$ -promoted SZ catalysts is not known, it should be negligible or at least much lower than that on HZSM-5 under the experimental conditions selected in this work due to much larger irregular pores and relatively much lower surface area of the catalysts. That means that the absolute activation energy for H/D exchange of methane on HZSM-5 will exceed 35% that of SZ,  $SZ/Al_2O_3$ , and SZA.

The similarity in absolute activation energy for the H/D exchange of methane on SZ,  $SZ/Al_2O_3$ , and SZA indicates that the acid strengths of unpromoted and  $Al_2O_3$ -promoted SZ samples are of the same order of magnitude. Based on the S=O stretching frequency shift of IR band before and after water or pyridine adsorption, Gao *et al.* (14, 15) claimed that the acid strengths of  $SZ/Al_2O_3$  and SZA catalysts are almost the same as that of SZ. The larger absolute activation energy on HZSM-5 in comparison with SZ-based samples seems to imply that the acid strength of HZSM-5 is weaker than those of the latter samples. According to the next nearest neighbour (NNN) theory stating that the intrinsic acid strength of an acid site is dependent on the number of Al atoms in the NNN position, decreasing the Al content is thought to increase the acidity of the bridging hydroxyl groups. Therefore, HZSM-5 (Si/Al = 39) employed for comparison in this contribution has the maximum acid strength among the HZSM-5 series samples with different Si/Al ratios (16, 27). Nevertheless, the true nature of the transition state, in particular its ionicity, is very much dependent on the environment of the active site, especially in a concerted process. Ab initio calculation at the highest level on the H/D exchange process between methane and the strongest liquid superacids shows that, even in these

TABLE 2

Kinetic Parameters of H/D Exchange between Methane and Deuterated Catalysts

Catalyst	Exchange rate <sup>a</sup> ( $10^{-9} \text{ mol (g}_{\text{cat}})^{-1} \text{ s}^{-1}$ )	$E_{\text{apparent}}$ ( $\text{kJ mol}^{-1}$ )	Temp. region (°C)
SZ	1.44	93	375–450
$SZ/Al_2O_3$	3.22	96	375–450
SZA	9.58	94	325–400
HZSM-5 <sup>b</sup>	3.95	129	375–450

<sup>a</sup> At 375°C.

<sup>b</sup> Si/Al = 39.

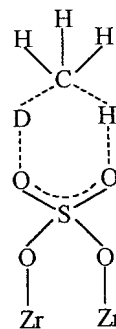
media, the mechanism is concerted and the environmental factor is important (28).

Sulfated zirconia possesses unique acid catalytic activity, and its low-temperature activity for hydrocarbon isomerization is well documented, especially for the isomerization of *n*-butane to isobutane, a hydrocarbon used in the production of oxygenates and alkylates. However, the acid strength of sulfated zirconia is still open to debate. On one hand, it has been claimed that SZ has superacidic acid sites or very strong acid sites (29–32). On the other hand, earlier use of Hammett indicators (“the visual method”), making SZ a strong solid superacid having  $H_0$  of  $-14.5$  to  $-16.0$ , is considered to be unreliable (33). Some reports have concluded that SZ is not a superacid and that its acidity is similar to that of HY but less than that of HZSM-5 (34–37). Our results, based on the H/D exchange of methane, indicate that the acidity of SZ is greater than that of HZSM-5. Therefore, we suggest that SZ may possess very strong acid sites. More recently, based on the kinetics of catalytic conversion of isobutane, Fraenkel (38) proposed that SZ may be a very strong solid superacid. Another study reported that the acid strength of SZ is higher than those of  $\text{Cs}_{2.5}\text{H}_{0.5}\text{PW}_{12}\text{O}_{40}$  heteropolyacid and zeolites such as HY, HZSM-5, and HMOR based on the activation energy of Ar desorption from these solid acids determined by TPD at lower temperatures (39). However, the point is that there is no clear definition of solid superacidity, and we have recently shown that due to the large scale of superacidity ( $-22 \leq H_0 \leq -12$ ) even different liquid superacids may behave differently toward alkanes (40).

An absolute activation energy of  $151 \text{ kJ mol}^{-1}$  for the H/D exchange of methane on HZSM-5 obtained in this work is in good accordance with both the findings of Schoofs *et al.* (16) and the previously reported theoretical value of  $150 \pm 20 \text{ kJ mol}^{-1}$  that was calculated based on a concerted reaction mechanism (41). It has been suggested in the theoretical model that the transition state for the H/D exchange between methane and acidic zeolites at higher temperatures is a “penta-coordinated carbonium ion” (41–45). Considering that the time dependence of isotopolog distribution is similar on both HZSM-5 and sulfated zirconia-based catalysts, we suppose that the transition state for the H/D exchange of methane over unpromoted and  $\text{Al}_2\text{O}_3$ -promoted SZ catalysts may also be a “penta-coordinated carbonium ion”, as shown in Scheme 1. The bisulfate species ( $\text{HSO}_4^-$ ) on the surface of sulfated zirconia-based samples are considered to act as strong Brønsted acid sites. In fact, this structural model of surface sulfate was proposed by various authors (29, 46–49).

### 3.3. Isomerization Reaction of *n*-Butane and Isobutane

In our earlier paper (50) we showed the stabilizing effect of hydrogen on the activity of SZ for *n*-butane isomerization. If the hydrogen pressure is high enough, the presence



SCHEME 1. Transition state for the H/D exchange of methane over SZ-based catalysts.

of platinum is not necessary to maintain the catalyst activity. To limit the deactivation of the catalysts, we have investigated *n*-butane and isobutane isomerization over our catalysts under a  $\text{H}_2$  atmosphere, keeping the hydrogen partial pressure at 690 Torr.

Table 3 shows the product selectivity of unpromoted and  $\text{Al}_2\text{O}_3$ -promoted SZ catalysts for *n*-butane isomerization at  $250^\circ\text{C}$  after the initial 10 min and after 360 min on stream. The main reaction product is isobutane, and the main by-products are propane and pentane. There is also a small quantity ( $\leq 1.7\%$ ) of methane and ethane produced during the isomerization of *n*-butane at high temperature. It is well known that sulfated zirconia-based catalysts can isomerize *n*-butane to isobutane with high selectivity. During the reaction the selectivity to isobutane for all catalysts is higher than 84% and exceeds 90% in the period of steady state. The small increase in selectivity to isobutane during the steady state compared with the initial period is related to the decrease in catalytic activity. *n*-Butane conversion over HZSM-5 gives only 25.0% selectivity to isobutane after 10 min on stream (not shown). The main reaction is cracking, yielding  $\text{C}_2$  and  $\text{C}_3$  fragments.

Figure 4 depicts the *n*-butane isomerization activity of unpromoted and  $\text{Al}_2\text{O}_3$ -promoted SZ catalysts with time on stream at  $250^\circ\text{C}$ . Fast deactivation is observed during

TABLE 3  
Product Selectivity for *n*-Butane Isomerization at  $250^\circ\text{C}$   
over Unpromoted and  $\text{Al}_2\text{O}_3$ -Promoted SZ Catalysts

Catalyst	Time (min)	Total rate ( $10^{-7} \text{ mol (g}_{\text{cat}})^{-1} \text{ s}^{-1}$ )	Selectivity (%)					
			$\text{C}_1$	$\text{C}_2$	$\text{C}_3$	i- $\text{C}_4$	i- $\text{C}_5$	<i>n</i> - $\text{C}_5$
SZ	10	8.46	0.2	0.7	4.0	91.5	2.6	1.0
	360	7.19	0.2	0.8	2.9	93.5	1.8	0.8
SZ/ $\text{Al}_2\text{O}_3$	10	13.54	0.4	0.9	5.3	89.6	2.9	0.9
	360	9.56	0.3	1.1	3.2	93.0	1.9	0.5
SZA	10	16.93	0.5	1.2	9.2	84.2	3.7	1.2
	360	12.27	0.4	1.3	5.0	89.4	2.8	1.1

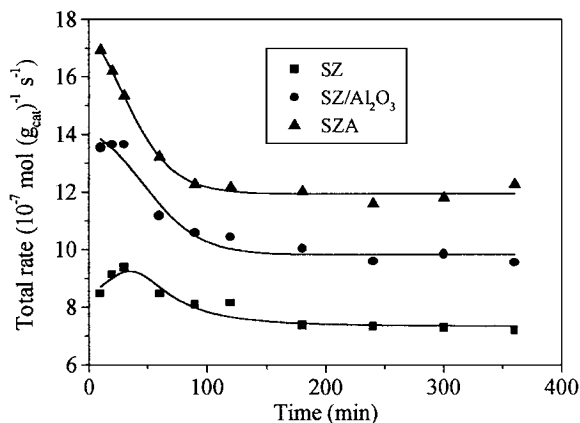


FIG. 4. Activity of unpromoted and  $\text{Al}_2\text{O}_3$ -promoted SZ catalysts for *n*-butane isomerization as a function of time at  $250^\circ\text{C}$ .

the initial 2 h on stream, after which all catalysts deactivate much more slowly and tend to reach steady activity. More recently, Kim *et al.* (51) suggested the possible presence of two types of active sites for *n*-butane isomerization on SZ. Taking into account the results published by other authors (14, 52), we think that the strong acid sites on sulfated zirconia-based catalysts contribute to the initial high activity for the isomerization of *n*-butane, whereas the intermediate strong acid sites are responsible for the steady activity. In view of both the initial and steady state activities of the catalysts, we can rate the catalyst activity as  $\text{SZA} > \text{SZ}/\text{Al}_2\text{O}_3 > \text{SZ}$ . The initial rate of *n*-butane conversion on HZSM-5 (not shown) is only  $5.3 \times 10^{-9} \text{ mol (g}_{\text{cat}})^{-1} \text{ s}^{-1}$  (corresponding to 0.15% conversion), which is 0.3 to 0.6% as large as those of unpromoted and  $\text{Al}_2\text{O}_3$ -promoted SZ catalysts.

Table 4 shows the product selectivity of unpromoted and  $\text{Al}_2\text{O}_3$ -promoted SZ catalysts for isobutane isomerization at  $250^\circ\text{C}$  after the initial 10 min and after 360 min on stream. The selectivity to *n*-butane for all catalysts during isobutane isomerization is also high ( $\geq 84.8\%$ ), but slightly lower than the selectivity to isobutane during *n*-butane isomerization at a comparable conversion level. Propane and pentane are

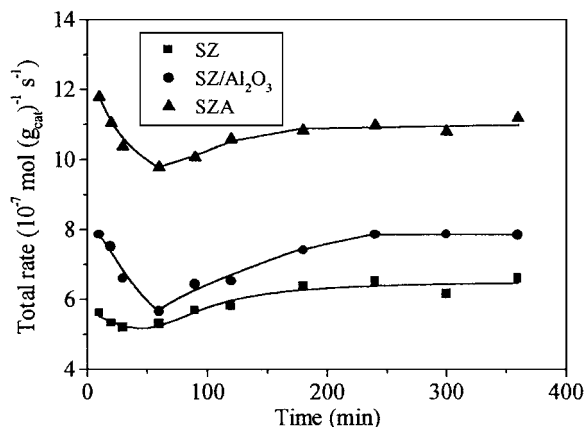


FIG. 5. Activity of unpromoted and  $\text{Al}_2\text{O}_3$ -promoted SZ catalysts for isobutane isomerization as a function of time at  $250^\circ\text{C}$ .

the main by-products, and traces of methane and ethane ( $\leq 1.1\%$ ) are also observed during isobutane isomerization on sulfated zirconia-based catalysts at high temperature in the presence of hydrogen. In the case of isobutane conversion over HZSM-5 (not shown), the main reaction products are propane and pentane, and the selectivity to *n*-butane is only 15.0% (10 min on stream).

Figure 5 presents the isobutane isomerization activity of unpromoted and  $\text{Al}_2\text{O}_3$ -promoted SZ catalysts with time on stream at  $250^\circ\text{C}$ . Interestingly, different from the feature during *n*-butane isomerization, the activity for isobutane isomerization over all catalysts first declines with time on stream and then increases to a steady value. The steady state rate of isobutane conversion is close to the initial one. At this point, the rate of catalyst deactivation is much slower during isobutane isomerization than during *n*-butane isomerization under the selected conditions, which may be due to the fact that during the isomerization of isobutane the coke precursors are more difficult to form (53). Moreover, the removal of coke precursor species is more effective since isobutane is known to be a better hydride transfer agent. Both the initial and steady state activities of the catalysts for isobutane isomerization are in the order of  $\text{SZA} > \text{SZ}/\text{Al}_2\text{O}_3 > \text{SZ}$ , showing the same sequence as those during *n*-butane isomerization. The higher rates of *n*-butane and isobutane conversion over  $\text{Al}_2\text{O}_3$ -promoted SZ catalysts than over SZ are caused by an enhancement of strong and intermediate strong acid sites (14, 15). In this study, we found that the rate of isobutane conversion is lower than that of *n*-butane conversion for the same catalyst, especially in the initial period of the reaction. A similar feature was observed by Fogash *et al.* (53) on SZ catalyst in the presence of helium. On the other hand, HZSM-5 zeolite (not shown) is much less active for the isomerization of isobutane than sulfated zirconia-based catalysts, giving an initial rate of  $2.2 \times 10^{-8} \text{ mol (g}_{\text{cat}})^{-1} \text{ s}^{-1}$  (corresponding to 0.62% conversion). Different from the

TABLE 4

Product Selectivity for Isobutane Isomerization at  $250^\circ\text{C}$  over Unpromoted and  $\text{Al}_2\text{O}_3$ -Promoted SZ Catalysts

Catalyst	Time (min)	Total rate ( $10^{-7} \text{ mol (g}_{\text{cat}})^{-1} \text{ s}^{-1}$ )	Selectivity (%)					
			$\text{C}_1$	$\text{C}_2$	$\text{C}_3$	<i>n</i> - $\text{C}_4$	i- $\text{C}_5$	<i>n</i> - $\text{C}_5$
SZ	10	5.61	0.4	0.1	5.9	88.8	4.8	0
	360	6.59	0.4	0.2	6.1	88.4	4.9	0
SZ/ $\text{Al}_2\text{O}_3$	10	7.86	0.5	0.3	6.0	87.7	4.6	0.9
	360	7.83	0.5	0.3	5.9	88.8	4.5	0
SZA	10	11.78	0.6	0.5	7.5	84.8	5.3	1.3
	360	11.18	0.5	0.4	6.1	87.2	4.6	1.2

behavior over unpromoted and  $\text{Al}_2\text{O}_3$ -promoted SZ catalysts, HZSM-5 zeolite is more active for isobutane conversion than for *n*-butane conversion. This is consistent with the results reported by Bearez *et al.* (54) over mordenites and by Engelhardt (55) over mordenites and Y zeolites.

The much higher selectivity for the isomerization of *n*-butane and isobutane over sulfated zirconia-based catalysts than over HZSM-5 zeolite may be related to the stronger acid character of the former catalysts. The sequence of the H/D exchange rate of methane over unpromoted and  $\text{Al}_2\text{O}_3$ -promoted SZ catalysts is the same as that of *n*-butane and isobutane conversion. Therefore, for the sulfated oxide catalysts one can use the rate of H/D exchange of methane to predict their activities for the isomerization of *n*-butane and isobutane. The difference between the H/D exchange rate of methane and the activities for *n*-butane and isobutane isomerization over HZSM-5 zeolite indicates that the acid sites participating in the former reaction are weaker than those taking part in the latter reactions.

#### 4. CONCLUSION

In the present work we have shown that the apparent activation energy for the H/D exchange reaction between methane and unpromoted or  $\text{Al}_2\text{O}_3$ -promoted SZ catalysts is identical within the experimental error, but substantially lower than that on HZSM-5 zeolite. Considering that the adsorption heat of methane on these sulfated zirconia-based catalysts should be negligible or at least much less than that on HZSM-5 under the experimental conditions employed, we conclude that the acidity of  $\text{Al}_2\text{O}_3$ -promoted SZ catalysts is the same as that of SZ, but greater than that of HZSM-5. However, the relationship of acidity with exchange rate should also take into account the environment of the active site and further work on a variety of catalysts might bring more information on this point.

A comparison of the behavior between the isomerization of *n*-butane and isobutane over unpromoted and  $\text{Al}_2\text{O}_3$ -promoted SZ catalysts shows that these catalysts deactivate more slowly during isobutane isomerization than during *n*-butane isomerization. The rate of isobutane conversion over SZ, SZ/ $\text{Al}_2\text{O}_3$ , and SZA catalysts follows the same order as that of *n*-butane conversion, i.e.,  $\text{SZA} > \text{SZ}/\text{Al}_2\text{O}_3 > \text{SZ}$ . For the same catalyst, it is more active during *n*-butane isomerization than during isobutane isomerization, especially in the initial period of the reaction. The agreement between the variation of the rates of H/D exchange of methane and the isomerization of *n*-butane and isobutane with the samples suggests that the H/D exchange reaction of methane may be useful as a probe to assess the relative acidity and reactivity of sulfated oxide catalysts.

#### ACKNOWLEDGMENTS

We thank Pr. J. Martens for providing HZSM-5 zeolite and Pr. F. Garin for fruitful discussions. We kindly acknowledge financial support from the Loker Hydrocarbon Institute, Los Angeles.

#### REFERENCES

1. Pines, H., "The Chemistry of Catalytic Hydrocarbon Conversion." Academic Press, New York, 1981.
2. Olah, G. A., Prakash, S. K., and Sommer, J., "Superacids." Wiley, New York, 1985.
3. Hino, M., Kobayashi, S., and Arata, K., *J. Am. Chem. Soc.* **101**, 6439 (1979).
4. Arata, K., *Adv. Catal.* **37**, 165 (1990).
5. Yamaguchi, T., *Appl. Catal.* **61**, 1 (1990).
6. Davis, B. H., Keogh, R. A., and Srinivasan, R., *Catal. Today* **20**, 219 (1994).
7. Corma, A., *Chem. Rev.* **95**, 559 (1995).
8. Song, X., and Sayari, A., *Catal. Rev.-Sci. Eng.* **38**, 329 (1996).
9. Hong, Z., Fogash, K. B., and Dumesic, J. A., *Catal. Today* **51**, 269 (1999).
10. Hollstein, E. J., Wei, J. T., and Hsu, C. Y., U.S. Patents 4,918,041, 4,956,519 (1990).
11. Hsu, C. Y., Heimbuch, C. R., Armes, C. T., and Gates, B. C., *J. Chem. Soc. Chem. Commun.* 1645 (1992).
12. Adeeva, V., de Haan, J. W., Janchen, J., Lei, G. D., Schunemann, V., van de Ven, L. J. M., Sachtler, W. M. H., and van Santen, R. A., *J. Catal.* **151**, 364 (1995).
13. Miao, C. X., and Gao, Z., *Chem. J. Chinese Univ.* **18**, 424 (1997).
14. Gao, Z., Xia, Y. D., Hua, W. M., and Miao, C. X., *Top. Catal.* **6**, 101 (1998).
15. Lei, T., Xu, J. S., Hua, W. M., Tang, Y., and Gao, Z., *Catal. Lett.* **61**, 213 (1999).
16. Schoofs, B., Martens, J. A., Jacobs, P. A., and Schoonheydt, R. A., *J. Catal.* **183**, 355 (1999).
17. Yamaguchi, T., Tanabe, K., and Kung, Y. C., *Mater. Chem. Phys.* **16**, 67 (1986).
18. Babou, F., Coudurier, G., and Vedin, J. C., *J. Catal.* **152**, 341 (1995).
19. O'Conneide, A., and Gault, F. G., *J. Catal.* **37**, 311 (1975).
20. Danyanova, S., Grange, P., and Delmon, B., *J. Catal.* **168**, 421 (1997).
21. Djuricic, B., Pickering, S., Glaude, P., McGarry, D., and Tambuyser, P., *J. Mater. Sci.* **32**, 589 (1997).
22. Eder, F., Stockenhuber, M., and Lercher, J. A., *J. Phys. Chem.* **101**, 5414 (1997).
23. Lercher, J. A., and Seshan, K., *Curr. Opin. Solid State Mater. Sci.* **2**, 57 (1997).
24. Denayer, J. F., Baron, G. V., Martens, J. A., and Jacobs, P. A., *J. Phys. Chem.* **102**, 3077 (1998).
25. Stach, H., Lohse, U., Thamm, H., and Schirmer, W., *Zeolites* **6**, 74 (1986).
26. McCullen, S. B., Reischman, P. T., and Olson, D. H., *Zeolites* **13**, 640 (1993).
27. Barthomeuf, D., *Stud. Surf. Sci. Catal.* **38**, 177 (1988).
28. Ahlberg, P., Karlsson, A., Goepfert, A., Nilsson Lill, S., Dinér, P., and Sommer, J., *Chem. Eur. J.*, in press.
29. Riemer, T., Spielbauer, D., Hunger, M., Mekhemer, G. A. H., and Knozinger, H., *J. Chem. Soc. Chem. Commun.* 1181 (1994).
30. Corma, A., Fornes, V., Juanrajadell, M. I., and Nieto, J. M. L., *Appl. Catal.* **116**, 151 (1994).
31. Morterra, C., Verrato, G., Pinna, F., Signoretto, M., and Strukul, G., *J. Catal.* **149**, 181 (1994).

32. Yaluris, G., Larson, R. B., Kobe, J. M., Gonzalez, M. R., Fogash, K. B., and Dumesic, J. A., *J. Catal.* **158**, 336 (1996).
33. Farcasiu, D., Ghenciu, A., and Li, J. Q., *J. Catal.* **158**, 116 (1996).
34. Cheung, T. K., d'Itri, J. L., Lange, F. C., and Gates, B. C., *Catal. Lett.* **31**, 153 (1995).
35. Kustov, L. M., Kazansky, V. B., Figueras, F., and Tichit, D., *J. Catal.* **150**, 143 (1994).
36. Adeeva, V., de Haan, J. W., Janchen, J., Lei, G. D., Schunemann, V., van de Ven, L. J. M., Sachtler, W. M. H., and van Santen, R. A., *J. Catal.* **151**, 364 (1995).
37. Drago, R. S., and Kob, N., *J. Phys. Chem.* **101**, 3360 (1997).
38. Fraenkel, D., *Chem. Lett.* 917 (1999).
39. Matsuhashi, H., and Arata, K., *Chem. Commun.* 387 (2000).
40. Goeppert, A., and Sommer, J., *Catal. Lett.* **56**, 43 (1998).
41. Kramer, G. J., van Santen, R. A., Emeis, C. A., and Nowak, A. K., *Nature* **363**, 529 (1993).
42. Kazansky, V. B., *J. Mol. Catal.* **74**, 257 (1992).
43. Kazansky, V. B., Frash, M. V., and van Santen, R. A., *Catal. Lett.* **28**, 211 (1994).
44. Kassab, E., Fouquet, J., Allavena, M., and Evleth, E. M., *J. Phys. Chem.* **97**, 9034 (1993).
45. Evleth, E. M., Kassab, E., and Sierra, L. R., *J. Phys. Chem.* **98**, 1421 (1994).
46. Saur, O., Bensitel, M., Saad, A. B. M., Lavalley, J. C., Tripp, C. P., and Morrow, B. A., *J. Catal.* **99**, 104 (1984).
47. Morterra, C., Cerrato, G., Pinna, F., and Signoretto, M., *J. Phys. Chem.* **98**, 12373 (1994).
48. Clearfield, A., Serrette, G. P. D., and Khazi-Syed, A. H., *Catal. Today* **20**, 295 (1994).
49. Zhao, E., Isaev, Y., Sklyarov, A., and Fripiat, J. J., *Catal. Lett.* **60**, 173 (2000).
50. Garin, F., Andriamasinoro, D., Abdulsamad, A., and Sommer, J., *J. Catal.* **131**, 199 (1991).
51. Kim, S. Y., Goodwin, J. G., Jr., and Galloway, D., *Catal. Lett.* **64**, 1 (2000).
52. Fogash, K. B., Yaluris, G., Gonzalez, M. R., Ouraipryvan, P., Ward, D. A., Ko, E. I., and Dumesic, J. A., *Catal. Lett.* **32**, 241 (1995).
53. Fogash, K. B., Hong, Z., Kobe, J. M., and Dumesic, J. A., *Appl. Catal.* **172**, 107 (1998).
54. Bearez, C., Chevalier, F., and Guisnet, M., *React. Kinet. Catal. Lett.* **22**, 405 (1983).
55. Engelhardt, J., *J. Catal.* **164**, 449 (1996).